Aquacultural Engineering 74 (2016) 111–119

Contents lists available at ScienceDirect

Aquacultural Engineering

journal homepage: www.elsevier.com/locate/aqua-online

Numerical simulation of deformations and forces of a floating fish cage collar in waves

Xiao-Hua Huang[a,b,*], Gen-Xi Guo[b], Qi-You Tao[b], Yu Hu[b], Hai-Yang Liu[b], Shao-Min Wang[b], Shuang-Hu Hao[c]

[a] Key Lab. of South China Sea Fishery Resources Exploitation & Utilization, Ministry of Agriculture, Guangzhou 510300, China
[b] South China Sea Fisheries Research Institute, Chinese Academy of Fishery Sciences, Guangzhou 510300, China
[c] Offshore Oil Engineering Company Limited, Tianjin 300452, China

ARTICLE INFO

Article history:
Received 10 March 2016
Received in revised form 17 July 2016
Accepted 25 July 2016
Available online 27 July 2016

Keywords:
Floating fish cage collar
Elastic deformation
Mooring line tension
Numerical simulation

ABSTRACT

The dynamic behavior of a fish cage collar in waves was investigated using a numerical model based on the finite element method. The floating collar and mooring system were divided into a series of line segments modeled by straight massless model segments with a node at each end. To verify the validity of the numerical model, research data from other authors were cited and compared with the simulated results, the comparison of results showed a good agreement. The numerical model was then applied to a dynamic simulation of a floating cage collar in waves to analyze its elastic deformation and mooring line tension. The simulated results indicated that the greatest deformation of the collar taken place in the position of the mooring line connection point when incident waves were in the same direction. An increase in the length of mooring line would help to decrease the mooring line tension of the collar. Furthermore, the effects of collar dimension, including collar circumference, pipe diameter in cross-section, and pipe thickness, on the dynamic behavior of the floating collar were discussed. The results of this study provided a better understanding of the dynamic behavior of the fish cage collar.

1. Introduction

Commercial marine fish farming is becoming prevalent in the world due to diminishing fishery resources in the ocean and increasing demand of sea products. As one of the main culture methods, cage aquaculture plays an important role in marine fish farming in China, of which yield accounts for about 50% of marine fish farming. Marine cage aquaculture has become an alternative for future development of the fisheries industry in China. However, owing to the aggravation of near-shore pollution and occupation of the sea area for coastal industrialization and tourism, cage farming locations need to be moved further offshore in exposed water. Therefore, the safety performance and reliability of the fish cage under the action of severe sea loads becomes the focus of attention.

In an open-sea area, a fish cage exposed to strong waves and current may deform to such a large extent that normal functionality is disabled. Therefore, extensive studies of hydrodynamic behaviors of fish cages have been conducted over the recent years. For example, Lee et al. (2008) presented a mathematical model for analyzing the performance of a fish cage with a floating collar influenced by currents and waves. Huang et al. (2008) analyzed the effects of waves with a uniform current on marine aquaculture gravity-type cages using a numerical model validated by physical model tests. A risk analysis (Huang and Pan, 2010) and submergence characteristics (Shainee et al., 2013) of single-point mooring cage system in waves and current were conducted. Kristiansen and Faltinsen (2012, 2015) proposed and discussed a screen type of force model for the viscous hydrodynamic load on an aquaculture net cage. Fredriksson et al. (2007a) studied mooring system tensions of a large fish farm containing 20 net pens in the absence of waves, using a numerical model and field measurements. Zhao et al. (2009, 2013) conducted analysis of dynamic behavior of a box-shaped net cage and a column-shaped net cage in waves and current using a numerical model, based on the lumped mass method and the principle of rigid body kinematics. DeCew et al. (2013) reported that an acoustic method was utilized to monitor the movement and deformation of a small-scale fish cage deployed in currents, and results were compared with field measurements.

* Corresponding author at: South China Sea Fisheries Research Institute, Chinese Academy of Fishery Sciences, No. 231 Xingangxi Road, Guangzhou 510300, China.
E-mail address: huangx-hua@163.com (X.-H. Huang).

http://dx.doi.org/10.1016/j.aquaeng.2016.07.003
0144-8609/

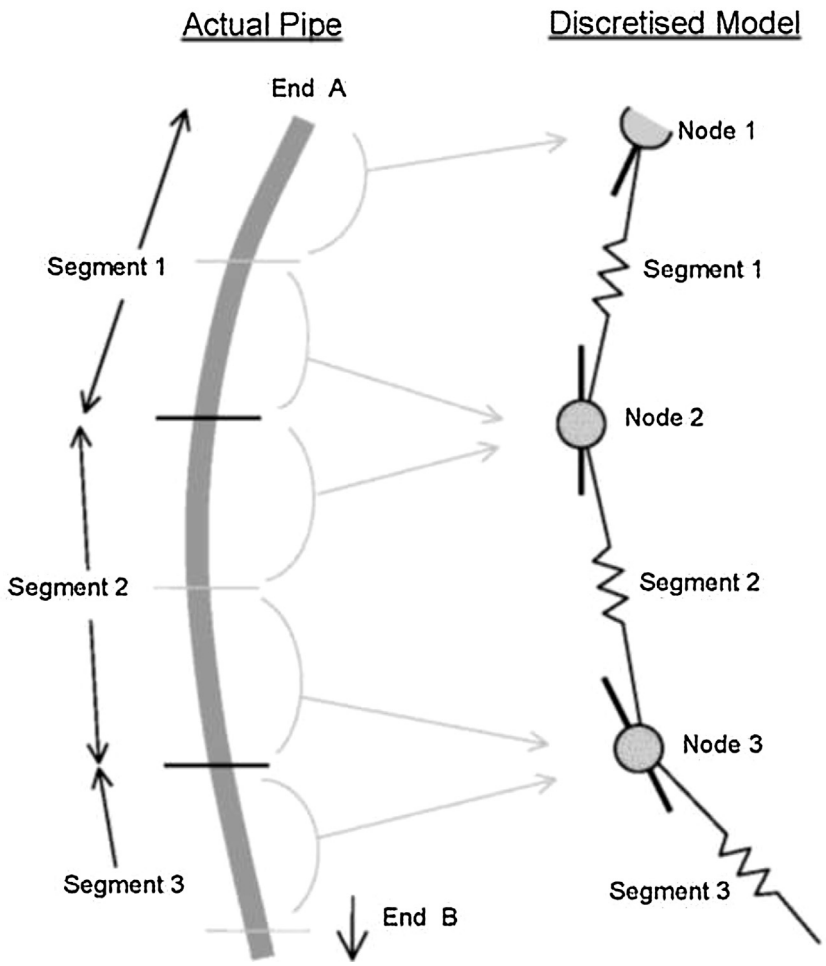

Fig. 1. A finite element model for the line.

Most of the aforementioned work is, however, based on the assumption that the load-bearing component floating collar of the fish cage is rigid, undergoing no deformations. Actually a floating fish cage collar made of high-density polyethylene (HDPE) may have great deformations resulting from strong winds and waves. Site observations have confirmed that the deformations of larger fish cages are more severe than those of smaller one. Therefore, deeply understanding the deformations of a floating collar is of vital importance to the reliable design of a fish cage with high security. Dong et al. (2010) and Hao (2008) analyzed the in-plane and out-of-plane deformations of a flotation ring of a gravity fish cage based on curved beam theory, in which the flotation ring was simplified into a circular ring. Fredriksson et al. (2007b) predicted the critical loading of net pen flotation structures using finite element modeling techniques, and conducted a series of experiments by testing circular sections of HDPE pipe to localized failure for the modeling approach. Li et al. (2013) studied dynamic responses of the semi-immersed floater and the fish cage system consisting of the floater and nets in waves and currents, in which large geometric deformations and motions were observed in both floater and the nets.

The objective of this paper is to analyze the deformations and forces of a floating fish cage collar subjected to pure waves. The study also considers effects of collar dimension on the deformations and forces of the fish cage collar. This paper is organized as follows. Section 2 introduces the numerical model of the fish cage collar. To validate the numerical model, two cases of circular pipe described in Hao (2008) and Li et al. (2013) are simulated and compared with the results from their works in Section 3. Afterwards, in Section 4, the numerical model is used to simulate the elastic deformations and the mooring line tensions of the floating collar in waves, and the effects of collar circumference, pipe diameter and pipe thickness are also analyzed. Finally, in Section 5, some conclusions are given.

2. Description of numerical model

2.1. Finite element model

A finite element model for a line is used to model the floating collar and mooring system of the fish cage. As shown in Fig. 1, the line is divided into a series of line segments which are then modeled by straight massless model segments with a node at each end. The model segments only model the axial properties of the line. The other properties (mass, weight, buoyancy, etc.) are all lumped towards the nodes, as indicated by the arrows in Fig. 1. The bending properties of the line are represented by rotational spring-dampers at each end of the segment, between the segment and the node. Each node is effectively a short straight rod that represents the two half-segments either side of the node. Forces and moments, including weight, buoyancy, hydrodynamic drag, tension and shear, bending, etc., are applied at the nodes. The equation of motion for each line node is as follows:

$$M(p, a) + C(p, v) + K(p) = F(p, v, t) \quad (1)$$

where $M(p, a)$ is the system inertia load, $C(p, v)$ is the system damping load, $K(p)$ is the system stiffness load, $F(p, v, t)$ is the external

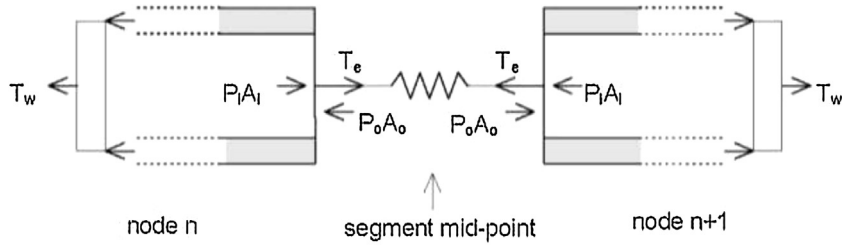

Fig. 2. Tension and pressure forces of the pipe structure.

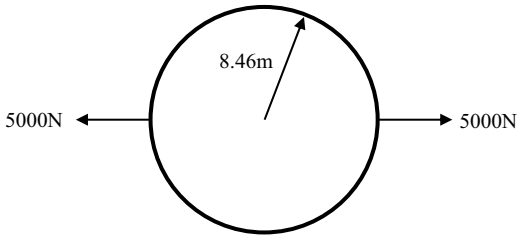

Fig. 3. Concentrated loads on the in-plane of the circular pipe.

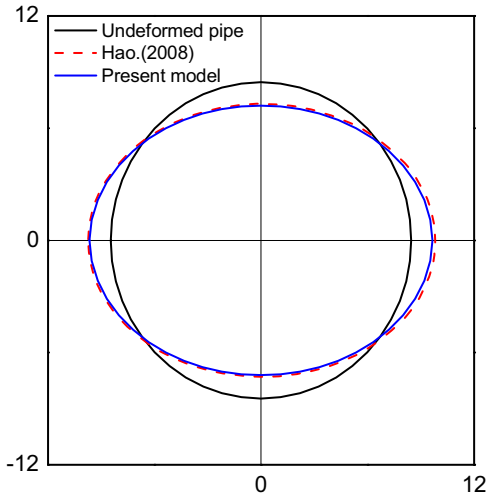

Fig. 4. Comparison of deformed shape to the pipe under concentrated loads.

load, t is the simulation time, p, v and a are the position, velocity, acceleration vectors respectively.

2.2. Structural loads

Generally, for the collar made with HDPE pipe, the total structural loads include tension forces, bend moments and shear forces, which resulting from the movements and deformations of the fish cage collar influenced by waves. It is assumed that the torsional effects are ignored for each line model of collar structure. For the mooring lines connecting the collar, the structural load is only tension forces, considering that the bend stiffness is insignificant, which can be set to zero. The effective tension of each line segment for the collar and mooring line structure is calculated together using the formula:

$$T_e = T_w + (P_0A_0 - P_iA_i) \tag{2}$$

In the equation, T_w represents the wall tension that can be written by:

$$T_w = EA\varepsilon - 2\mu\,(P_0A_0 - P_iA_i) + EAC\left(dL/dt\right)/L_0 \tag{3}$$

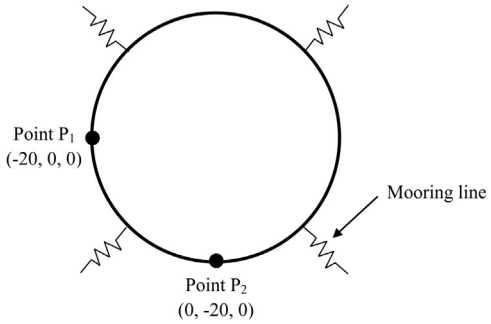

Fig. 5. Sketch of the circular pipe model for calculations.

where EA is axial stiffness of line, ε is total mean axial strain that is given by $(L–L_0)/L_0$, L and L_0 are instantaneous length and unstretched length of segment, μ is Poisson ratio, P_i and P_0 are internal and external (i.e. surrounding fluid) pressure, A_i and A_0 are internal and external cross-sectional stress areas (see Fig. 2), C is damping coefficient, dL/dt is rate of increase of length. For the mooring lines of fish cage, T_e is equal to T_w.

The bend moment of line segment for modeling collar structure is given by:

$$M = EIk + kd\left(\lambda_b/100\right)D_c/dt \tag{4}$$

where EI is bending stiffness of a segment, k is curvature, λ_b is target bending damping, D_c is the bending critical damping value for a segment, which is given by $L_0(mEIL_0)^{1/2}$. The node experiences two bend moments, M_1 and M_2, one from the segments on each side of it.

Having calculated the bend moments at each end of the segment, the shear force in the segment can be calculated. Because the model segment is stiff in bending, the bend moment varies linearly along the segment and shear force in the segment is the constant vector equal to the rate of change of bend moment along the length. The shear force is therefore given by:

$$Q = S_Z \times (M_2 - M_1)/L \tag{5}$$

where S_Z is unit vector in the segment axial direction, L is the instantaneous length of the segment.

2.3. Hydrodynamic loads

An extended form of Morison's equation (Morison et al., 1950) is used to calculate hydrodynamic loads on each line segment of the floating collar and mooring lines structure. There are two force components, one related to water particle velocity, the drag force, and one related to water particle acceleration, the inertia force. The inertia force consists of two parts, one proportional to water particle acceleration, and one proportional to water particle accel-

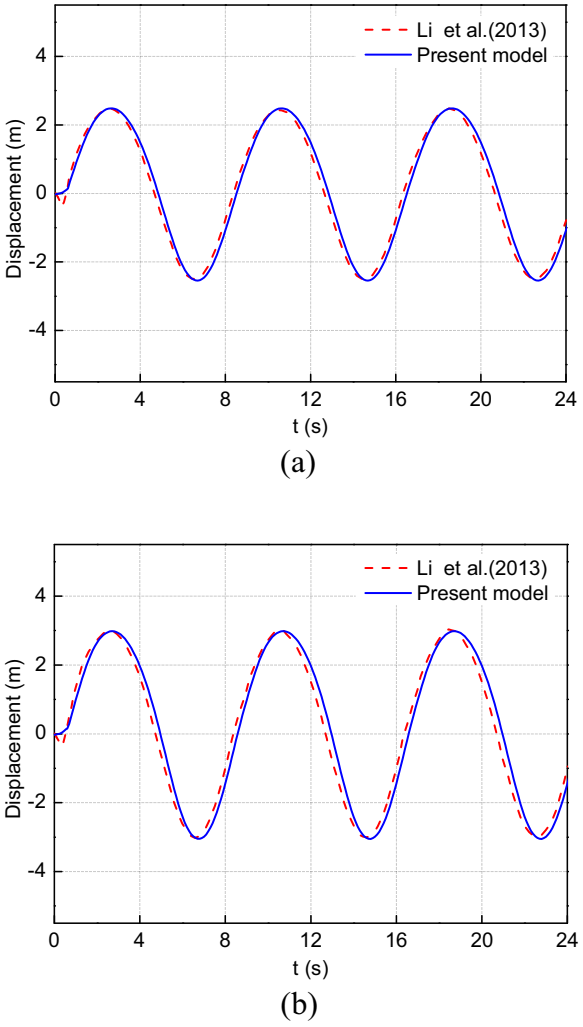

Fig. 6. Comparison of vertical displacement of point P_1 at (a) wave height H = 5 m and (b) wave height H = 6 m.

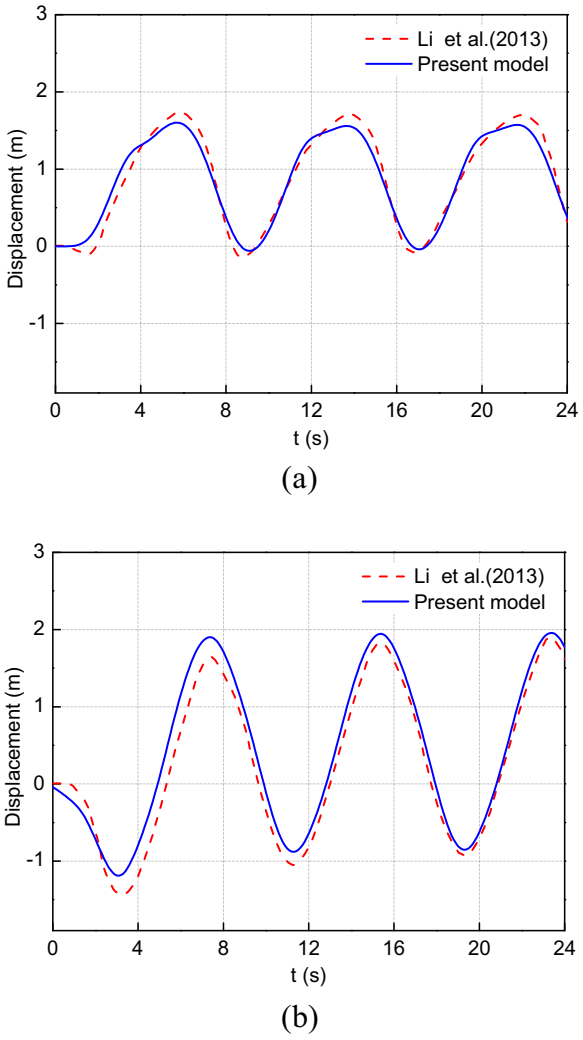

Fig. 7. Comparison of displacement of point P_2 in (a) x direction and (b) y direction.

eration relative to the line segment. The extended form of Morison's equation is as follows:

$$F_W = \frac{1}{2}\rho C_d S V_r |V_r| + \rho \forall a_f + \rho \forall C_a a_r \quad (6)$$

where F_W denote the fluid force, ρ is the density of water, S is the drag area, V_r is the water particle velocity relative to the segment, $\forall$ is the volume of water displaced by the segment, a_f is the water particle acceleration, a_r is the water particle acceleration relative to the segment, C_d and C_a are the drag coefficient and the added mass coefficient. Here C_d and C_a are set to 1.2 and 1.0, respectively.

2.4. Numerical algorithm method

As described previously, each mid-node experiences two tension forces, two bend moments, two shear forces (one each from the segments either side of the node). These loads are then combined with other non-structural loads such as weight, buoyancy (this is given by $\rho g \forall$) and hydrodynamic loads, etc. to give the total force and moment on the node. Afterwards, Eq. (1) is solved for the acceleration vector, for each line node, and then integrated using semi-implicit Euler integration with a constant time step (Orcina Ltd., 2015). Then the values of the velocity and position at each node at time t+1, are given by:

$$v_{t+1} = v_t + a_t dt \quad (7)$$

$$p_{t+1} = p_t + v_{t+1} dt \quad (8)$$

where dt is the time step. At the end of each time step, the positions and orientations of all line nodes and segments are again known and the process is repeated. In this study, a commercial program, OrcaFlex (Orcina Ltd., 2015), is chosen to accomplish the dynamic analysis.

3. Model validations

To examine the validity of the numerical model, deformation data of circular pipe under concentrated loads from Hao (2008) and motion data of circular pipe in waves from Li et al. (2013) are cited and compared with the simulated results using the model.

3.1. Validation 1 (deformations of circular pipe under concentrated loads)

The first validation case is chosen to calculate the deformations of circular pipe, from the work done by Hao (2008). For the numerical calculation, we use the parameters of Hao's (2008) circular pipe: the radius of the pipe is 8.46 m, and the cross-sectional radius is

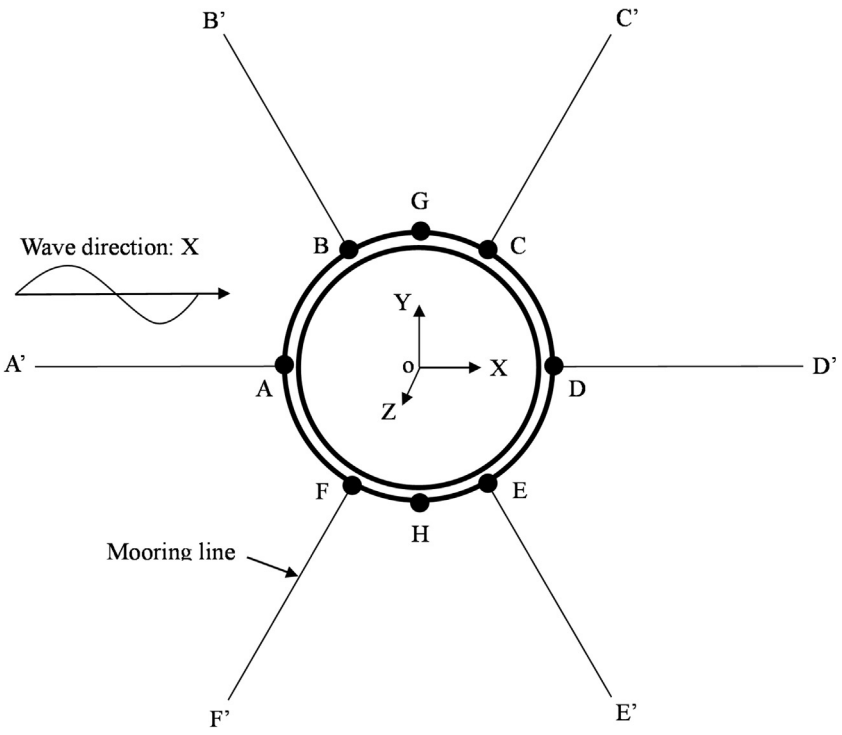

Fig. 8. The configuration of the floating fish cage collar.

Table 1
Properties of the floating collar for calculations.

Parameter	Value
Circumference	60 m
Outer diameter of pipe	0.315 m
Wall thickness	0.019 m
Material	HDPE
Density	953 kg/m^3
Modulus of elasticity	950 MPa
Poisons ratio	0.42
Yield stress	24 MPa
Length of mooring line	60 m
Axial stiffness of mooring line	260 kN

Table 2
The deformation and displacement at different points of the floating collar.

Point of the collar	Displacement (m)			Max von Mises strain (%)	Max von Mises stress (MPa)
	x	y	z		
A (−10.10, 0.0, 0.0)	2.06	0.00	2.98	0.49	4.65
B (−5.05, 8.75, 0.0)	2.12	0.11	2.94	0.30	2.90
C (5.05, 8.75, 0.0)	2.08	0.14	3.04	0.17	1.60
D (10.10, 0.0, 0.0)	2.21	0.00	3.10	0.25	2.39
E (5.05, −8.75, 0.0)	2.08	0.14	3.04	0.17	1.60
F (−5.05, −8.75, 0.0)	2.12	0.11	2.94	0.30	2.90
G (0.0, 10.10, 0.0)	2.08	0.21	3.00	0.29	2.72
H (0.0, −10.10, 0.0)	2.08	0.21	3.00	0.29	2.72

0.125 m; the elastic modulus is 900 MPa. The concentrated loads of 5000 N act on two endpoints of the pipe, shown in Fig. 3.

Fig. 4 shows the shape of the circular pipe when it is placed in a horizontal plane and is exposed to concentrated loads of 5000 N. It can be seen that the deformed pipe computed from the present model almost coincide with that from Hao (2008), in which the relative errors of the maximum displacement in horizontal and vertical direction are all less than 5%.

3.2. Validation 2 (motions of circular pipe in waves)

The second validation case is chosen to calculate the motions of circular pipe in regular waves, from the work done by Li et al. (2013). In the research of Li et al. (2013), the floating circular pipe is connected by four mooring lines, which are simulated by nonlinear springs (see Fig. 5). A zero force is defined when the springs are under compression. The pipe is made of plastic with a density of 953 kg/m^3 and has a diameter of 40 m and an outer diameter of 0.3 m in cross-section. The thickness of the pipe is 0.048 m and the elastic modulus is 950 MPa. We select two points P_1 and P_2 marked in Fig. 5 to analyze the pipe motions and make a comparison with that obtained from Li et al. (2013). Wave heights of 5 m, 6 m and period of 8 s are utilized in the calculation.

Time histories of the vertical displacement of point P_1 on the floating pipe in regular waves are plotted in Fig. 6, and time histories of the displacement of point P_2 in x and y direction are plotted in Fig. 7. From Fig. 7, we can see that remarkable y direction displacement at point P_2 indicates a large structural deformation on the floating circular pipe in waves. As shown in Fig. 6 and 7, the calculated results obtained from the numerical model presented in Section 2 are all in close agreement with that obtained from Li et al. (2013), in which the largest relative error is only 6.5% for the maximum displacement of points P_1 and P_2. Based on the above analysis, the model is feasible in simulating the dynamic response of a circular pipe in waves.

4. Numerical simulation of the floating fish cage collar

Fig. 8 shows the configuration of the floating collar, which is connected by a six-point mooring system. The collar is simplified into two circular pipes in parallel with attachment connections. In the figure, points A–H are attachments points, and points A′–F′ are anchor points. The main properties of the floating collar are listed in Table 1. During the calculation, wave height, wave period and water depth are set to 6 m, 8 s and 20 m, respectively.

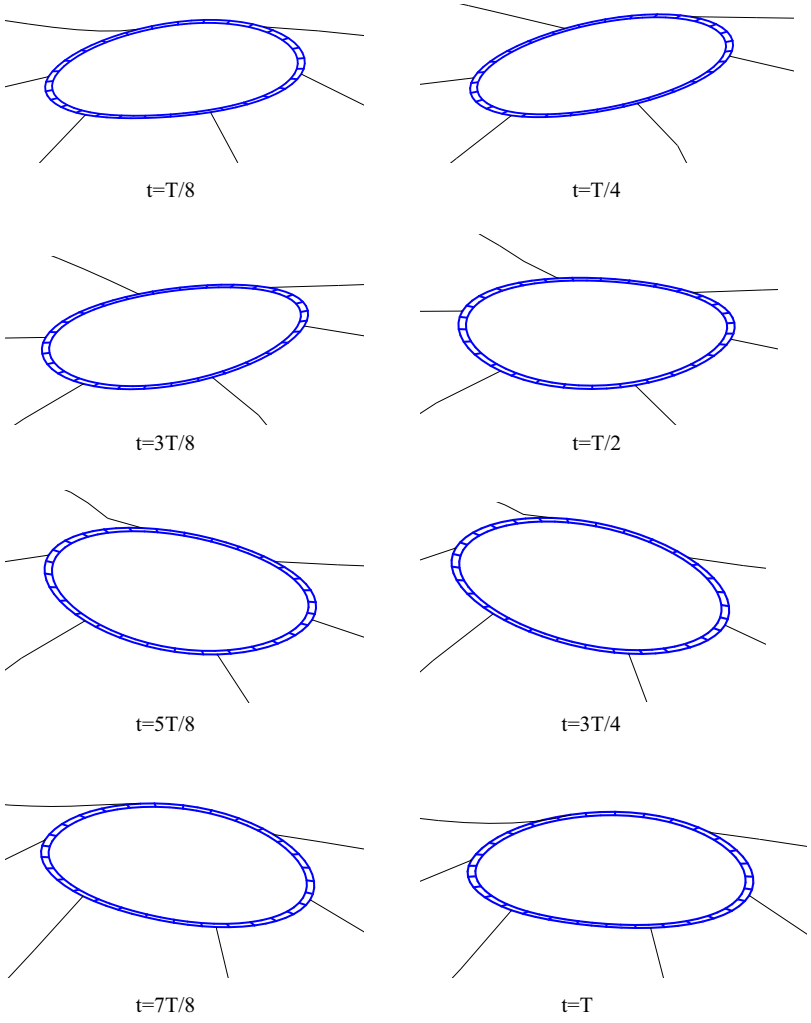

Fig. 9. Deformed shape of the floating collar in waves at different times.

4.1. Elastic deformation of the floating collar in waves

Fig. 9 shows the instantaneous deformed shape of the floating collar exposed to waves running in the positive x direction at different times during one wave period. It can be found that deformation occurs to the collar in waves at different times and the deformation is greater when t = T/2 and t = T than at other times. Hence the elasticity of the collar should be considered in the dynamic analysis of that (Endresen, 2011).

The deformation and displacement for each point position on the floating collar is provided in Table 2 where the von Mises strain ε_{vm} and stress σ_{vm} can be written as follows:

$$\varepsilon_{vm} = \sqrt{\varepsilon_{zz}^2 + \varepsilon_{cc}^2 - \varepsilon_{zz}\varepsilon_{cc}} \tag{9}$$

$$\sigma_{vm} = \sqrt{\frac{(\sigma_1 - \sigma_2)^2 + (\sigma_2 - \sigma_3)^2 + (\sigma_3 - \sigma_1)^2}{2}} \tag{10}$$

where ε_{zz} is the axial strain due to direct tensile strain and bending strain, ε_{cc} is the hoop strain and $\sigma_1, \sigma_2, \sigma_3$ are the principal stresses.

Among all points A–H of the collar, the von Mises strain of point A is the largest, and points B and F come second together because the mooring line AA′ has a greater tension due to the same direction of the incident waves. For the displacement in y direction, the value of points G and H are the largest, while the value of points A and D are zero due to the symmetry of the collar structure. For the von Mises stress, the largest value is much less than the yield stress of the HDPE pipe. Furthermore, the relationship of the von Mises strain and von Mises stress is given by Fig. 10. The analysis above reveals that the deformation of the collar is under the range of elastic deformation.

4.2. Mooring line tension of the floating collar in waves

It is known that the deformation of the fish cage collar is caused not only by waves, but also by mooring line tension. Mooring line tension is a high concern for the design of the fish cage collar and mooring system. Therefore, we conducted the calculation of mooring line tension of the floating collar in waves and the results are shown in Fig. 11. It can be observed that, among all mooring lines, the tension of mooring line AA′ is the largest, of which the peak value is about 11 kN. The tension of mooring line CC′ and EE′ are the same smallest, of which the peak value is only about 3 kN. Furthermore, at the bottom of each curve (see Fig. 11), tension is equal to zero, because mooring line is loose without bearing any compression.

To investigate the tension of mooring line with different length, three kinds of L/h = 3–5 are adopted where L denotes the length of mooring line and h is water depth. Assuming water depth is constant, which is equal to 20 m. The calculated results are provided in Fig. 12. We can see that the effect of L/h on mooring line tension is significant. The increase in L/h helps to decrease mooring line tension, which can further reduce the deformation of the collar from

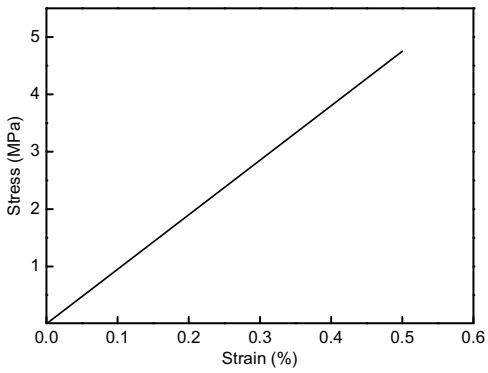

Fig. 10. The elastic deformation behavior of the floating collar.

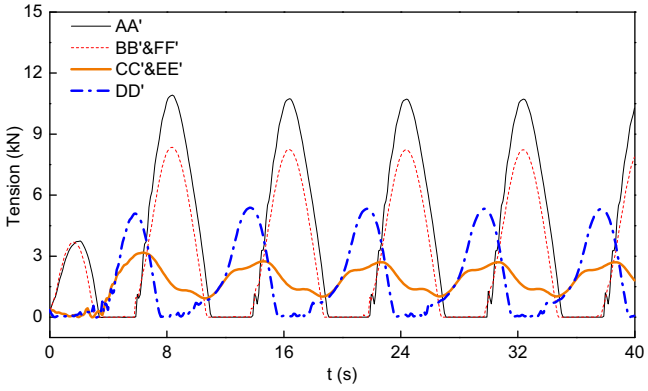

Fig. 11. Time-series of tension for different mooring lines.

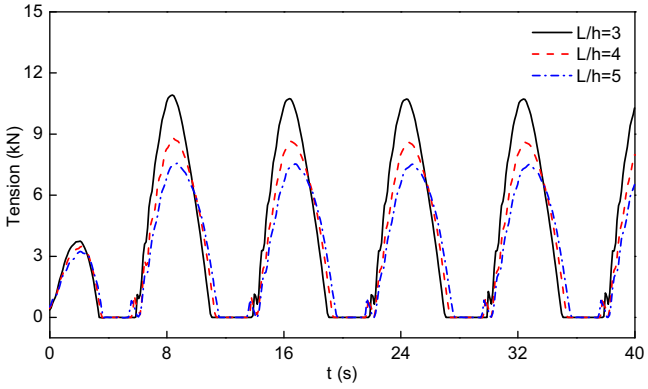

Fig. 12. Time-series of the mooring line tension for L/h = 3–5.

the analysis in Section 4.1. According to the simulation results, in reality, increasing the length of mooring line would help to enhance the performance of resisting natural risk to the fish cage in open sea.

4.3. *Effects of the floating collar dimension*

The deformation and force of the fish cage collar in waves has a close relationship with the dimension. Therefore, we chose to investigate the dimension impact of three collar circumferences (60, 80, and 100 m), various pipe diameters (from 0.25 to 0.45 m) in cross-section and pipe thickness (from 12.1 to 28.6 mm) on the deformation and force of floating collar exposed to waves, in which the deformation is expressed with the von Mises strain of point A and the force is expressed with the tension of mooring line AA′ (see Fig. 8).

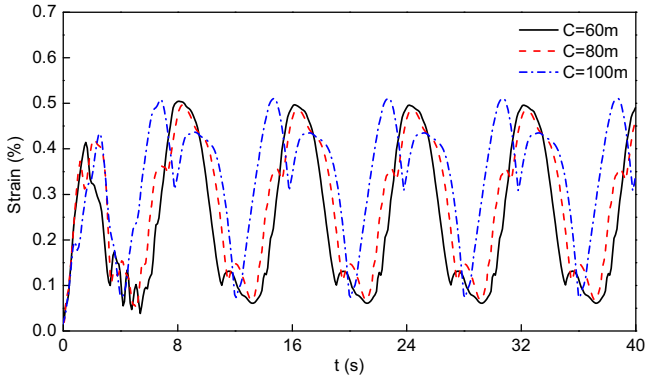

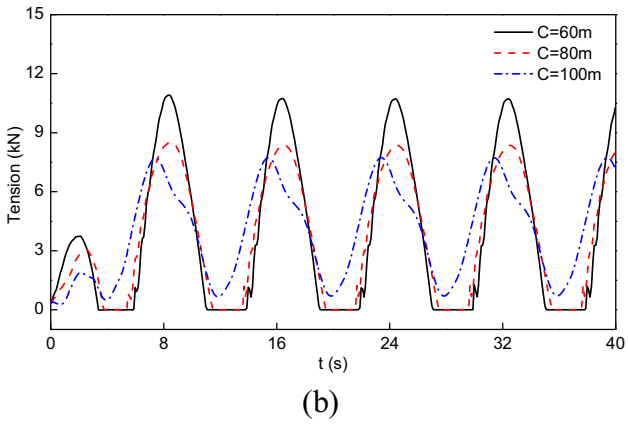

Fig. 13. Time-series of the (a) von Mises strain at point A and (b) mooring line tension of the collar with different circumferences.

As seen from Fig. 13a, under the same conditions, the maximum strain for collar with different circumferences has no significant change, which indicates the effect of collar circumference on deformation is small. For the mooring line tension, as shown in Fig. 13b, the effect of collar circumference is significant. The maximum mooring line tension reduces with an increasing circumference of collar at the same pipe parameters in cross-section. This is the reason that the increasing range of collar movement is much less than that of collar radius with incident waves. Similar results have been reported by Hao (2008).

Fig. 14 shows the calculated results of maximum strain and maximum mooring line tension with the variation of pipe diameter in cross-section. It can be seen that the strain decreases with an increasing outer diameter of pipe, whereas the trend of mooring line tension is opposite. As shown in Fig. 15, with an increasing pipe thickness, the strain decreases from 0.61% to 0.39% and the mooring line tension increases from 10.4 to 11.3 kN. The increasing range is relatively small for the mooring line tension, compared to that in Fig. 14.

5. Conclusions

This paper presents a numerical model based on the finite element method, for modeling the dynamic behavior of a fish cage collar in waves. The validity of the numerical model is verified by comparing the results with the data from Hao (2008) and Li et al. (2013). Using the numerical model, the elastic deformation and mooring line tension of a floating fish cage collar are analyzed and discussed in detail. Several primary conclusions are given as follows:

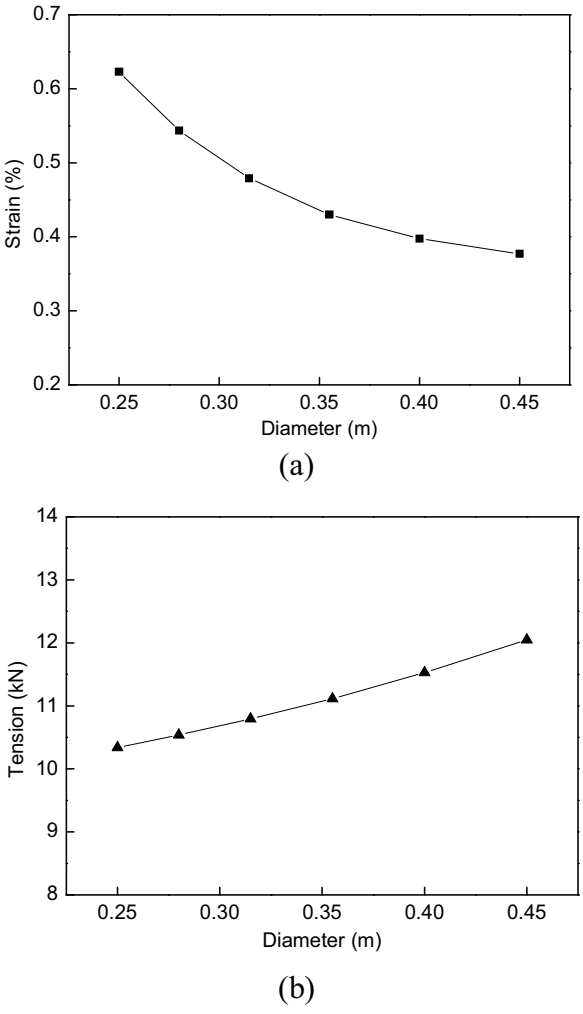

Fig. 14. Results of the deformation and force of the collar with different outer diameters of pipe at thickness of 0.0187 m. (a) Maximum von Mises strain, (b) Maximum mooring line tension.

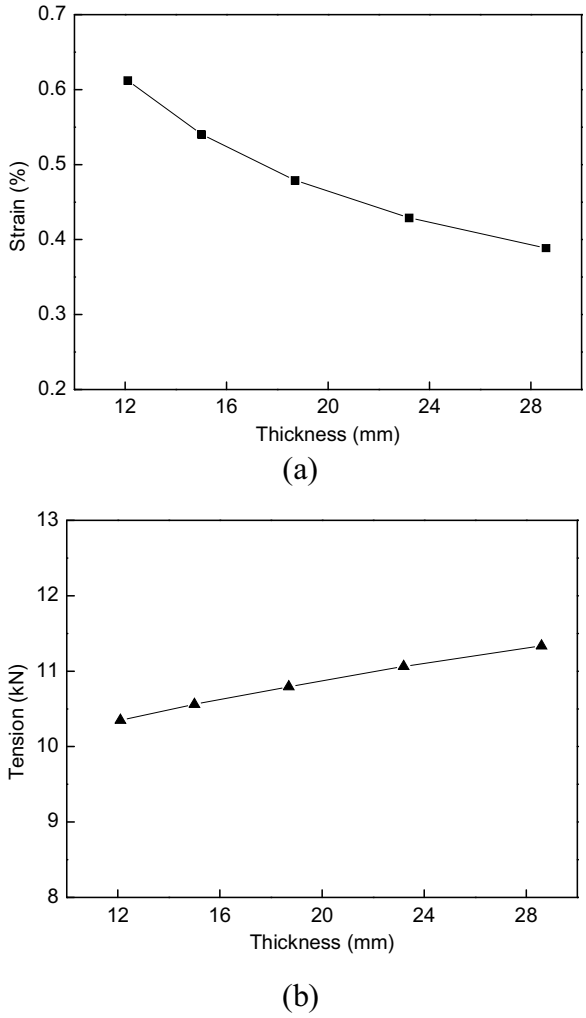

Fig. 15. Results of the deformation and force of the collar with different pipe thickness at outer diameter of 315 mm. (a) Maximum von Mises strain, (b) Maximum mooring line tension.

(1) The numerical model presented in this paper is suitable to simulate the dynamic behavior of a fish cage collar in waves.
(2) Deformation occurs to the floating collar in waves. The greatest deformation takes place in the position of the mooring line connection point when the incident waves are in the same direction.
(3) An increase in the length of mooring line helps to decrease mooring line tension.
(4) The effect of collar circumference on the maximum strain of the floating collar is small, but with increasing collar circumference the maximum mooring line tension decreases.
(5) With increasing cross-sectional diameter or thickness of pipe, the maximum strain of the floating collar becomes smaller and the maximum mooring line tension becomes larger.

Acknowledgements

This work was financially supported by the National Natural Science Foundation of China (Grant No. 31402349), Science and Technology Program of Guangdong Province (Grant No. 2013B020501001), Science and Technology Major Project of Hainan Province (Grant No. ZDKJ2016011), as well as Guangdong Innovation and Development of Regional Marine Economy Demonstration Project (Grant No. GD2013-D01-001).

References

DeCew, J., Fredriksson, D.W., Lader, P.F., Chambers, M., Howell, W.H., Osienki, M., Celikkol, B., Frank, K., Høy, E., 2013. Field measurements of cage deformation using acoustic sensors. Aquacult. Eng. 57 (6), 114–125.
Dong, G.H., Hao, S.H., Zhao, Y.P., Zong, Z., Gui, F.K., 2010. Elastic responses of a flotation ring in water waves. J. Fluids Struct. 26 (26), 176–192.
Endresen, P.C., 2011. Vertical wave loads and response of a floating fish farm with circular collar. In: Master Thesis. Norwegian University of Science and Technology, Norway.
Fredriksson, D.W., DeCew, J.C., Tsukrov, I., Swift, M.R., Irish, J.D., 2007a. Development of large fish farm numerical modeling techniques with in-situ mooring tension comparisons. Aquacult. Eng. 36 (2), 137–148.
Fredriksson, D.W., DeCew, J.C., Tsukrov, I., 2007b. Development of structural modeling techniques for evaluating HDPE plastic net pens used in marine aquaculture. Ocean Eng. 34 (16), 2124–2137.
Hao, S.H., 2008. The study of fluid-structure interaction of the flotation ring of a gravity-type fish cage. In: Ph.D. Dissertation. Dalian University of Technology, China.
Huang, C.C., Pan, J.Y., 2010. Mooring line fatigue: a risk analysis for an SPM cage system. Aquacult. Eng. 42 (1), 8–16.
Huang, C.C., Tang, H.J., Liu, J.Y., 2008. Effects of waves and currents on gravity-type cages in the open sea. Aquacult. Eng. 38 (2), 105–116.
Kristiansen, T., Faltinsen, O.M., 2012. Modelling of current loads on aquaculture net cages. J. Fluids Struct. 34 (4), 218–235.
Kristiansen, T., Faltinsen, O.M., 2015. Experimental and numerical study of an aquaculture net cage with floater in waves and current. J. Fluids Struct. 54, 1–26.
Lee, C.W., Kim, Y.B., Lee, G.H., Choe, M.Y., Lee, M.Y., Koo, K.Y., 2008. Dynamic simulation of a fish cage system subjected to currents and waves. Ocean Eng. 35 (14–15), 1521–1532.

Li, L., Fu, S.X., Xu, Y.W., Wang, J.G., Yang, J.M., 2013. Dynamic responses of floating fish cage in waves and current. Ocean Eng. 72 (7), 297–303.
Morison, J.R., O'Brien, M.D., Johnson, J.W., Schaaf, S.A., 1950. The force exerted by surface waves on piles. J. Petrol. Technol. 2 (5), 149–154.
Orcina Ltd., 2015. OrcaFlex Manual version 10.0a. Ulverston, Cumbria, UK.
Shainee, M., DeCew, J., Leira, B.J., Ellingsen, H., Fredheim, A., 2013. Numerical simulation of a self-submersible SPM cage system in regular waves with following currents. Aquacult. Eng. 54 (3), 29–37.
Zhao, Y.P., Li, Y.C., Dong, G.H., Gui, F.K., Teng, B., 2009. The numerical simulation of hydrodynamic behaviors of gravity cage in current and waves. Int. J. Offshore Polar Eng. 19 (2), 97–107.
Zhao, Y.P., Gui, F.K., Xu, T.J., Chen, X.F., Cui, Y., 2013. Numerical analysis of dynamic behavior of a box-shaped net cage in pure waves and current. Appl. Ocean Res. 39 (1), 158–167.